THE JOURNAL OF PHYSICAL CHEMISTRY LETTERS
A JOURNAL OF THE AMERICAN CHEMICAL SOCIETY

pubs.acs.org/JPCL

Letter

Pressure Gradient Squeezing Hydrogen out of MnOOH: Thermodynamics and Electrochemistry

Yida Wang, Xin Yang, Xingyu Tang, Xuan Wang, Yapei Li, Xiaohuan Lin, Xiao Dong, Dongliang Yang, Haiyan Zheng, Kuo Li,* and Ho-kwang Mao

Cite This: J. Phys. Chem. Lett. 2021, 12, 10893−10898

Read Online

ACCESS | Metrics & More | Article Recommendations | Supporting Information

ABSTRACT: Pressure of gigapascal (GPa) is a robust force for driving phase transitions and chemical reactions with negative volume change and is intensely used for promoting combination/addition reactions. Here, we find that the pressure gradient between the high-pressure region and the ambient-pressure environment in a diamond anvil cell is an even stronger force to drive decomposition/elimination reactions. A pressure difference of tens of GPa can "push" hydrogen out from its compounds in the high-pressure region to the environment. More importantly, in transition metal hydroxides such as MnOOH, the protons and electrons of hydrogen can even be separated via different conductors, pushed out by the high pressure, and recombine outside under ambient conditions, producing continuous current. A pressure-gradient-driven battery is hence proposed. Our investigation demonstrated that a pressure gradient is a special and powerful force to drive decomposition and electrochemical reactions.

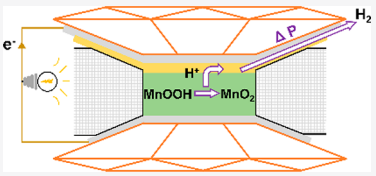

Juxtaposed with temperature, pressure acts as the other external thermodynamic variable that defines the stability and reactivity of substances.[1,2] Applying extremely high pressure (HP) successfully synthesized novel compounds and materials, such as superconductor LaH_{10} with T_c at 260 K under 180 GPa,[3] alkali halides $NaCl_3$ and Na_3Cl with unexpected stoichiometry,[4] and the high-energy-density material NaN_5, etc.[5] Considering the temperature effect is often secondary under pressure of gigapascal, the thermodynamic driving force under HP is described by the enthalpy change. As presented in Scheme 1, when substance A is compressed at 0 K, $dH = dU + d(PV) = T\,ds - P\,dV + V\,dP + P\,dV = V\,dP$, and the enthalpy contributed by external pressure is the integral of the equation of state (EOS) of A [$V_A(P)$] on the P-axis, $\Delta H_A|_{P0}^{P1} = \int_{P0=0}^{P1} V_A(P)\,dP$, as represented by the area between the EOS and the P-axis (inside the red boarder in Scheme 1). Similarly, for substance B, $\Delta H_B|_{P0}^{P1} = \int_{P0=0}^{P1} V_B(P)\,dP$ (line-shading in Scheme 1). For a transition A = B under pressure P_1 (in the scale of GPa) and T = 0 K, the enthalpy change of the reaction contributed by external pressure ($\Delta H_r|_{P0}^{P1}$) is the difference between these two integral (dot-shading), and finally the enthalpy change of the reaction at P_1, $\Delta H_{r,P1} = \Delta H_{r,P0} + \Delta H_r|_{P0}^{P1}$

$$= \Delta H_{r,P0} + \Delta H_B|_{P0}^{P1} - \Delta H_A|_{P0}^{P1}$$

where $\Delta H_{r,P0}$ is the enthalpy change of the reaction under P_0 = 0 GPa and T = 0 K. When it is negative, the reaction will proceed spontaneously. This is a natural conclusion from the equilibrium thermodynamics under isobaric conditions, and most of the high-pressure theoretical and experimental research is under such an isobaric assumption.

On the other hand, if a pressure gradient is involved, that is, (part of) the atoms under the HP (P_1, with volume V_1) chamber are "squeezed" to an ambient-pressure environment (P_0, with volume V_0), an additional enthalpy change must be considered. For example, when A under a HP chamber (P_1, with volume $V_{A,1}$) transfers to B in an ambient-pressure environment (P_0, with volume $V_{B,0}$), an additional term $\Delta H_B|_{P1}^{P0}$ equal to $-\Delta H_B|_{P0}^{P1}$ should be added; then the enthalpy change of the reaction

Scheme 1. Enthalpy Changes under Applied Pressure[a]

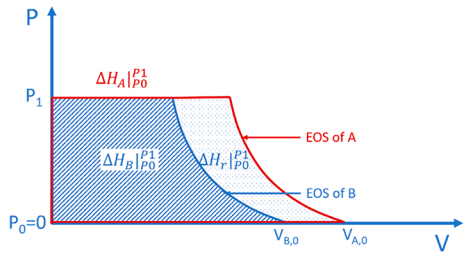

[a]EOS stands for equation of state, describing the P−V relationship.

Received: October 14, 2021
Accepted: October 28, 2021
Published: November 3, 2021

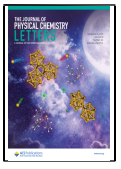

https://doi.org/10.1021/acs.jpclett.1c03382
J. Phys. Chem. Lett. 2021, 12, 10893−10898

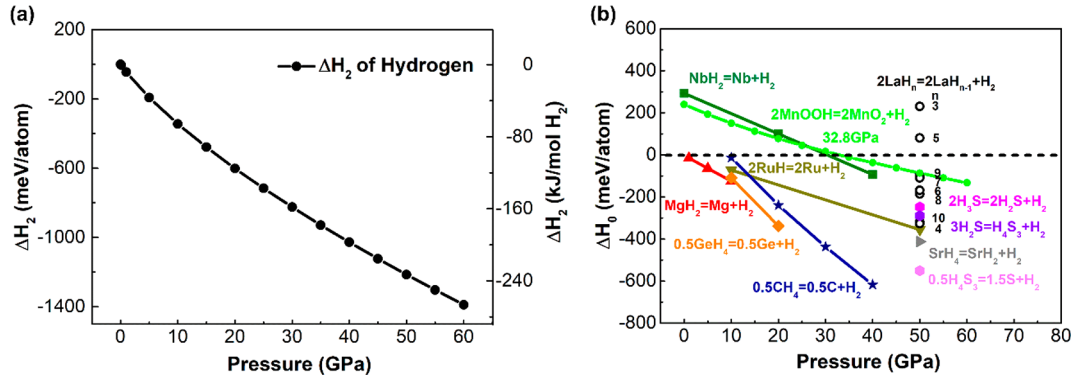

Figure 1. Enthalpy changes with hydrogen released from HP to 0 GPa. (a) HP H_2-ruler. (b) ΔH_0 of binary hydrides, where ΔH_0 is the sum of ΔH_1[8−16] and ΔH_2 (HP H_2-ruler), normalized by the number of atoms in the reaction.

$$\begin{aligned}\Delta H_r|_{A,P1}^{B,P0} &= \Delta H_{r,P0} + \Delta H_r|_{P0}^{P1} + \Delta H_B|_{P1}^{P0} \\ &= \Delta H_{r,P0} + \Delta H_B|_{P0}^{P1} - \Delta H_A|_{P0}^{P1} + \Delta H_B|_{P1}^{P0} \\ &= \Delta H_{r,P0} - \Delta H_A|_{P0}^{P1}\end{aligned}$$

Note that $\Delta H_A|_{P0}^{P1}$ corresponds to the whole integral area of the EOS of A on the P-axis, which is much larger than the $(\Delta H_A|_{P0}^{P1} - \Delta H_B|_{P0}^{P1})$ discussed above and can be even larger with increasing pressure. In a rough estimation, when an atom travels from a chamber at P_1 = 100 GPa to an environment at P_0 = 0 GPa, the enthalpy will decrease by ∼10 eV (∼10^3 kJ/mol, details in Table S1). This is high enough to break any chemical bonds and drive the physical/chemical transition. We can conclude that such a pressure gradient is more powerful than the isobaric external pressure and can be realized when the atoms are squeezed out from the HP chamber. This is possible for the reactions with gas eliminated, such as H_2, etc., and the pressure gradient can dominate the reaction process according to the above analysis.

In this work, we found that the hydrogen can be squeezed out from many hydrogen-bearing compounds (A-H) by theoretical calculation and thermodynamic analysis. Then in an experiment we successfully squeezed the hydrogen out from MnOOH by applying a pressure gradient of ∼30 GPa over hundreds of micrometers, as demonstrated by an *in situ* X-ray diffraction (XRD) experiment. More importantly, by physically separating the migration path of the protons and electrons, we built up a closed circuit and constructed a prototype of a pressure-gradient-driven battery, which generates current using a pressure gradient and hence coupled the pressure gradient with electrochemistry.

We first investigated several representative hydrogen-bearing compounds (A-H) including protonic compounds, covalent-bonded molecules, and metal hydrides theoretically. For the hydrogen-escaping, the initial state is A-H under HP and 0 K, and the final state is A under HP and hydrogen in an environment under 0 GPa. The whole process (0) is not in an equilibrium state and has to be decomposed into two virtual steps to calculate the enthalpy change, including an isobaric decomposition at pressure P_1 (1) and the escaping of H_2 from P_1 to P_0 = 0 GPa (2) as shown below. The corresponding enthalpy changes are noted as ΔH_0, ΔH_1, and ΔH_2, respectively, with $\Delta H_0 = \Delta H_1 + \Delta H_2$.

$$\text{A-H}\ (P_1) = \text{A}\ (P_1) + \text{H}_2\ (P_0) \qquad \Delta H_0 \qquad (0)$$

$$\text{A-H}\ (P_1) = \text{A}\ (P_1) + \text{H}_2\ (P_1) \qquad \Delta H_1 \qquad (1)$$

$$\text{H}_2\ (P_1) = \text{H}_2\ (P_0) \qquad \Delta \text{H}_2 \qquad (2)$$

Thermodynamically, the hydrogen would escape to the ambient environment if $\Delta H_0 = \Delta H_2 + \Delta H_1 < 0$. Here $\Delta H_2 = \int_{P1}^{P0=0} V_{H2}(P)\, dP$, which is a big negative value, and $|\Delta H_2|$ would increase significantly with increasing pressure. Even if ΔH_1 is positive, ΔH_0 will change from positive to negative at a critical pressure, and the whole process would therefore proceed spontaneously. ΔH_2 is calculated from P_1 = 0 to 60 GPa using CASTEP (Figure 1a), which can be used as a gauge (HP H_2-ruler) to compare to the ΔH_1 of various A-H and predict the critical pressure for reactions.

As a representative of protonic compounds, the ΔH_0 for γ-MnOOH was calculated under HP. It is selected because both γ-MnOOH and the expected product β-MnO_2 have a rutile structure. The escaping of hydrogen would not reconstruct the lattice and hence may facilitate the kinetics. More importantly, the proton may transport separately with electrons and have potential applications in electrochemistry, as discussed later in this paper. For 2γ-MnOOH = 2β-MnO_2 + H_2 under room temperature and 0 GPa, $\Delta_f G_m$(MnOOH) = −557.99 kJ·mol^{-1},[6] and $\Delta_f G_m$(MnO_2) = −465.40 kJ·mol^{-1},[7] so $\Delta_r G_m$(0 GPa) = $2[\Delta_f G_m(MnO_2) - \Delta_f G_m(MnOOH)]$ = 185.18 kJ·mol^{-1}, which indicates the decomposition is unfavorable. The enthalpy changes of MnOOH, MnO_2, and H_2 upon compression $\Delta H|_{P0=0}^{P1}$ were then calculated respectively (see Tables S2 and S3) and added to $\Delta_r G_m$ (P = 0 GPa) to simulate ΔH_1 (supposing the TS term and temperature effect are neglectable) under HP. ΔH_0 was obtained by adding the HP H_2-ruler (ΔH_2) to ΔH_1, as presented in Figure 1b. It predicts that MnOOH would decompose to MnO_2 above 32.8 GPa if H_2 can be released to ambient pressure. Then we also examined the ΔH_0 of several H-bearing compounds reported in the literature, including LaH_n, SrH_4, NbH_2, MgH_2, CH_4, etc., by subtracting the enthalpy of formation ($\Delta H_1 = -\Delta_f H_m$) under HP[8−16] from the HP H_2-ruler, as shown in Figure 1b. We found most ΔH_0 values become negative below 60 GPa, suggesting spontaneous escaping of H_2 under the pressure gradient.

Experimentally, we compressed MnOOH (synthetic process in the Supporting Information and XRD data in Figure S1) to 55 GPa using a diamond anvil cell (DAC) with a Pd gasket, which can transmit hydrogen and hence facilitate the H_2 elimination from γ-MnOOH. A pressure transmitting medium

https://doi.org/10.1021/acs.jpclett.1c03382
J. Phys. Chem. Lett. 2021, 12, 10893−10898

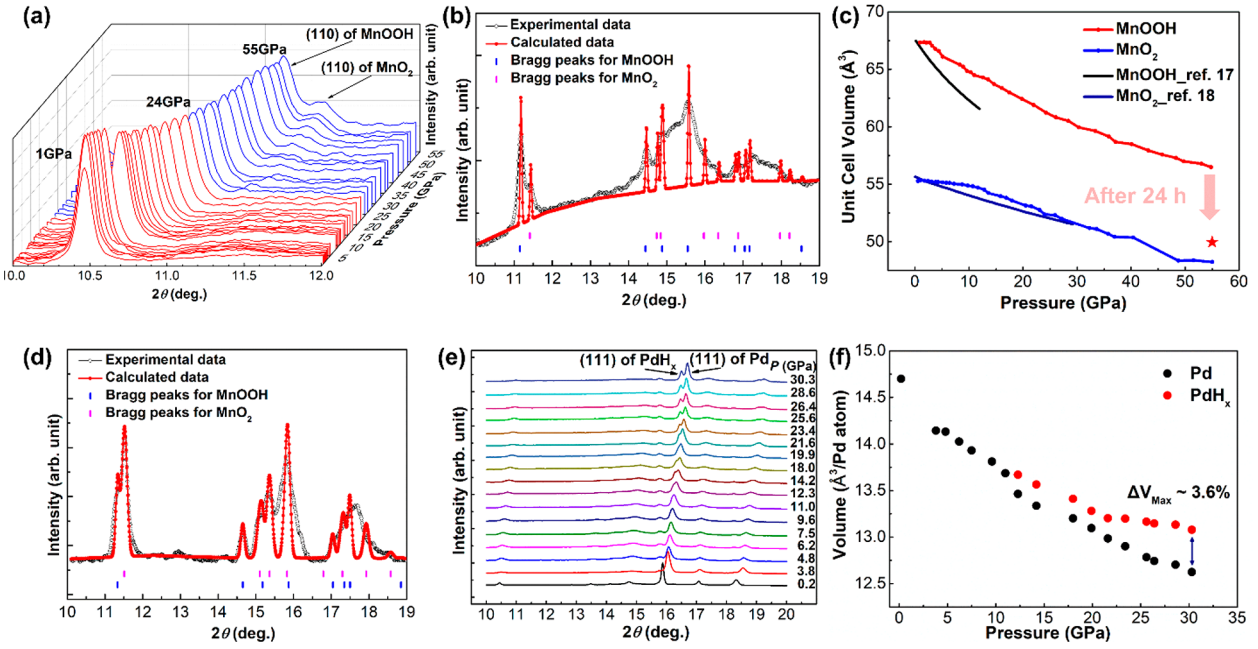

Figure 2. *In situ* high-pressure XRD investigations of MnOOH in a Pd gasket. (a) Selected XRD plots of γ-MnOOH from 1 to 55 GPa. (b) Simulated and experimental XRD patterns of γ-MnOOH and β-MnO_2 at 55 GPa. (c) Pressure−volume relationships of γ-MnOOH and β-MnO_2. The red star represents the unit cell volume of γ-MnOOH after staying at 55 GPa for ~24 h. (d) Simulated and experimental XRD patterns of γ-MnOOH and β-MnO_2 at ~55 GPa after ~24 h. (e) XRD data of Pd on the inner edge of the gasket. (f) Volume of Pd and PdH_x (per Pd atom) under high pressure. The maximum difference of the volume (3.6%) appears at 30 GPa.

is not used to guarantee the good contact between MnOOH and Pd. The selected *in situ* XRD data ($10° < 2\theta < 12°$) with increasing pressure is shown in Figure 2a (the complete XRD pattern is shown in Figure S2). Above 26 GPa, a new peak appears at the high-angle side of the 110 peak ($2\theta = 11°$), which is the 110 diffraction of β-MnO_2. At 55 GPa, the highest pressure in our investigation, the XRD data is well fitted by a mixture of γ-MnOOH (a = 4.182 Å, b = 4.931 Å, c = 2.739 Å, *Pnnm*) and β-MnO_2 (a = 4.420 Å, b = 4.400 Å, c = 2.865 Å, *Pnnm*), as shown in Figure 2b. This indicates that MnOOH partly transforms into β-MnO_2. Refining the lattice parameters under high pressure reveals the pressure−volume (P−V) relationships of γ-MnOOH, as represented by the red line in Figure 2c. The P−V curve of β-MnO_2 was also measured separately for reference (blue line), while the black line and royal blue line are the P−V curves of γ-MnOOH and β-MnO_2 from previous reports.[17,18] The red star in Figure 2c represents the volume of γ-MnOOH at ~55 GPa after ~24 h. It shrinks from the MnOOH curve toward the MnO_2 curve, indicating a huge volume collapse caused by gradually losing hydrogen over hours. Figure 2d presents the XRD pattern of the MnOOH and MnO_2 mixture staying at 55 GPa after 24 h, which shows the content of β-MnO_2 increases from 24.5 wt % to 60.5 wt % while that of γ-MnOOH decreases from 75.5 wt % to 39.5 wt %. The quantitative phase analysis is determined by the reference intensity ratio (RIR) method,[19] with RIR(MnOOH) = 3.63 [ICDD: 98-008-4949] and RIR(MnO_2) = 4.28 [ICDD: 98-005-6006]. The P−V curve in ref 17 (black line in Figure 2c) is from a large volume press (LVP) experiment. Typically, the sealing of the LVP is not as good as the DAC and the loading rate is slower, hence providing good admittance and more time for H_2 to escape. This is most likely why in their experiment the lattice shrinks more obviously upon compression and supports our conclusion.

The XRD data of the Pd gasket was also collected by illuminating the X-ray beam on the inner edge in contact with MnOOH (Figure 2e). The 111 peak of Pd begins to broaden above 12 GPa and then splits into two peaks above 23 GPa, which are recognized as Pd and PdH_x (Figure 2f), respectively, also indicating the hydrogen transport from MnOOH to Pd under high pressure. Hence, we can conclude that the hydrogen of MnOOH was squeezed out under the extreme pressure gradient.

Squeezing hydrogen out of γ-MnOOH under a pressure gradient is a decomposition process and is also a redox reaction, which can be coupled with a charge transport process. If the proton and electron of hydrogen escape from a high-pressure chamber through separated routes and recombine at ambient conditions, an electric current is produced. Hence, an electrochemical process can be designed as below:

Anode (under HP):

$$\mathrm{MnOOH} - \mathrm{e}^- = \mathrm{MnO_2} + \mathrm{H}^+ \quad (3)$$

Cathode (ambient):

$$\mathrm{H}^+ + \mathrm{e}^- = 1/2\mathrm{H_2} \quad (4)$$

Then, we made a pressure-gradient-driven battery (PGDB) to separate the proton and electron transports based on a diamond anvil cell (Figure 3). It contains four layers between the two diamonds, including a top Pt electrode (cathode), Nafion film (electrolyte), MnOOH (anode), and a bottom Pt electrode (photos in Figure S3). Pt is an excellent proton-blocking-electron-conducting electrode, while Nafion is proton-conducting-electron-blocking. When MnOOH tends to release H^+ and electrons under enough pressure gradient, its neighbor, Nafion, can only conduct protons, while the other neighbor Pt can only conduct electrons. Hence, protons would transfer through the Nafion film from the center to the edge

https://doi.org/10.1021/acs.jpclett.1c03382
J. Phys. Chem. Lett. 2021, 12, 10893−10898

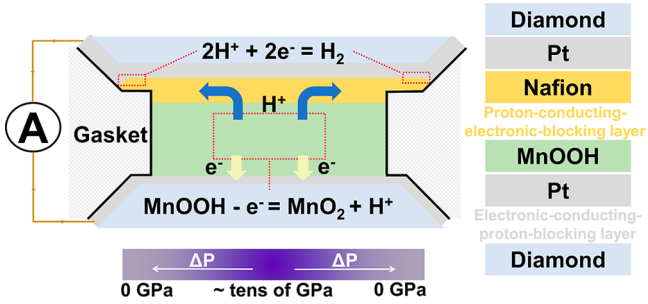

Figure 3. Schematic plot of the pressure-gradient-driven battery.

driven by the pressure gradient, electrons transport through the bottom Pt electrode and external circuit, and they recombine at the top Pt electrode and form H_2.

We used electrochemical impedance spectroscopy (EIS) to demonstrate the PGDB model. Figure 4a shows the Nyquist plots of the model up to 22.5 GPa, which contain a semicircle at high frequencies and a straight line at low frequencies. The straight line represents Warburg impedance because the proton diffuses through Nafion and is reduced between the Pt and Nafion interface. For reference, the settings without MnOOH or Nafion do not show such Warburg impedance (Figures S4 and S5) because there is no path for protons to escape continuously. Using the equivalent circuit method, we can obtain the corresponding resistance (10^6 Ω) and capacitance of the semicircle up to 22.5 GPa (Figure 4b). According to Irvine's interpretation,[20] the capacitance (~10^{-11} F/cm) of the semicircle is attributed to the grain boundary's impedance. During the whole compression process, the values were maintained in the same order of magnitude, which demonstrates the device's stability under high pressure.

More directly, the time-dependent direct current (DC) was measured with a picoammeter (for the reliability, see Figure S6) to demonstrate the PGDB model. Pd cathodes were used to help hydrogen to escape from the system quickly. Just as assumed, hundreds of picoamps were detected in the normal setting (for details see SI Electrical measurements) under applied pressure, showing the maximum value of the current at about 9 GPa (Figure 4c green line). Divided by the minuscule amount of MnOOH ($m = 2 \times 10^{-6}$ g), the peak current is ~0.3 mA/g, which is already a very intense signal. No current was detected in the reverse connection (switch the ± connection of the picoammeter, Figure 4d green line), which demonstrates the strategy of separating the electrons and protons. Some control-group experiments were also conducted for reference. When MnOOH was replaced by cubic boron nitride (BN), no current was detected up to 30 GPa (Figure S7), indicating that the 10^2 of picoamps of current we observed in Figure 4c indeed resulted from MnOOH. When MnOOH is replaced by another piece of Nafion (much thicker than the electrolyte Nafion under compression) with a top Pd electrode (cathode) and a bottom Pt electrode (anode), a much weaker current is observed and decays more quickly under high pressure (Figure 4c and d yellow line). This shows that Nafion can only provide a very limited amount of protons, not really contribute to the current signal of MnOOH.

In summary, with theoretical and experimental investigation, we found that the pressure gradient can drive the elimination of hydrogen from various hydrogen-bearing compounds, including metal hydrides and hydroxide like γ-MnOOH. Quantitatively, a HP H_2-ruler is presented to measure the pressure under which a hydrogen-bearing compound can release hydrogen. Based on this process, we designed a pressure-gradient-driven battery by physically separating the transferring routes of protons and electrons, as demonstrated

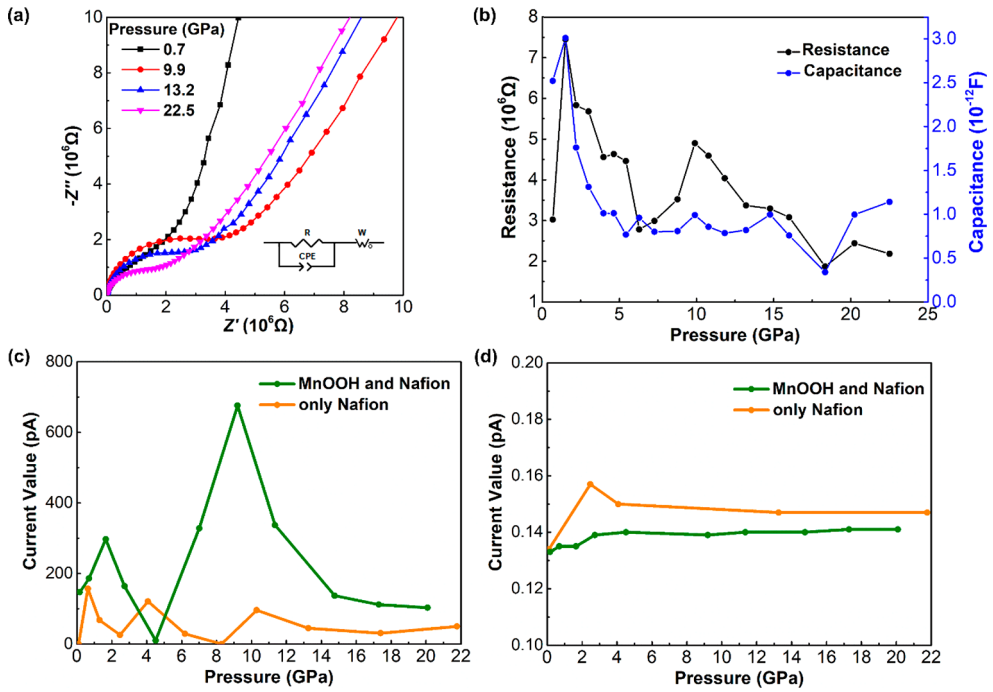

Figure 4. (a) EIS of the MnOOH-PGDB at high pressure in the Nyquist plot. The inset shows the equivalent circuit. (b) Resistance and capacitance of the MnOOH-PGDB during compression. (c) DC values of the MnOOH-PGDB, in the normal and (d) reverse connection for reference.

https://doi.org/10.1021/acs.jpclett.1c03382
J. Phys. Chem. Lett. 2021, 12, 10893−10898

by EIS and DC measurements. Our work directly transfers mechanical energy to electrical energy under a huge pressure gradient and can potentially be realized under extreme conditions deep underground or in the giant planet.

■ ASSOCIATED CONTENT

Supporting Information

The Supporting Information is available free of charge at https://pubs.acs.org/doi/10.1021/acs.jpclett.1c03382.

Details of materials preparation, measurement methods, and supplementary figures (Figure S1−S7) and tables (Tables S1−S3) including the sample preparation, *in situ* high-pressure synchrotron X-ray diffraction, electrical measurements, density-functional theory (DFT) computational details, estimation of enthalpy change when an atom travels from high pressure to ambient pressure, XRD of MnOOH under applied pressure, photos of the insulated gasket, impedance spectroscopy of MnOOH and Nafion in the Nyquist plot under applied pressure, the reliability of the picoammeter, PGDB model filling with an insulator, and the structures of H_2, γ-MnOOH, and β-MnO_2 (PDF)

■ AUTHOR INFORMATION

Corresponding Author

Kuo Li − *Center for High Pressure Science and Technology Advanced Research, 100094 Beijing, China;* orcid.org/0000-0002-4859-6099; Email: likuo@hpstar.ac.cn

Authors

Yida Wang − *Center for High Pressure Science and Technology Advanced Research, 100094 Beijing, China*

Xin Yang − *Center for High Pressure Science and Technology Advanced Research, 100094 Beijing, China*

Xingyu Tang − *Center for High Pressure Science and Technology Advanced Research, 100094 Beijing, China*

Xuan Wang − *Center for High Pressure Science and Technology Advanced Research, 100094 Beijing, China*

Yapei Li − *Center for High Pressure Science and Technology Advanced Research, 100094 Beijing, China*

Xiaohuan Lin − *Center for High Pressure Science and Technology Advanced Research, 100094 Beijing, China*

Xiao Dong − *Key Laboratory of Weak-Light Nonlinear Photonics, School of Physics, Nankai University, 300071 Tianjin, China*

Dongliang Yang − *Institute of High Energy Physics, Chinese Academy of Sciences, 100049 Beijing, China*

Haiyan Zheng − *Center for High Pressure Science and Technology Advanced Research, 100094 Beijing, China;* orcid.org/0000-0002-4727-5912

Ho-kwang Mao − *Center for High Pressure Science and Technology Advanced Research, 100094 Beijing, China*

Complete contact information is available at: https://pubs.acs.org/10.1021/acs.jpclett.1c03382

Notes

The authors declare no competing financial interest.

■ ACKNOWLEDGMENTS

This research was made possible as a result of a generous grant from the National Natural Science Foundation of China (NSFC) (Grant nos. 22022101, 21771011, and 21875006) and the National Key Research and Development Program of China (2019YFA0708502). This research used resources of the BL15U1 beamline at the Shanghai synchrotron radiation facility and 4W2 beamline at the Beijing synchrotron radiation facility. The author acknowledges Xujie Lü for helpful discussion.

■ REFERENCES

(1) Mao, H. K.; Chen, B.; Chen, J.; Li, K.; Lin, J. F.; Yang, W.; Zheng, H. Recent Advances in High-Pressure Science and Technology. *Matter Radiat. at Extremes* **2016**, *1*, 59−75.

(2) Yang, X.; Wang, X.; Wang, Y.; Li, K.; Zheng, H. From Molecules to Carbon Materials—High Pressure Induced Polymerization and Bonding Mechanisms of Unsaturated Compounds. *Crystals* **2019**, *9*, 490.

(3) Somayazulu, M.; Ahart, M.; Mishra, A. K.; Geballe, Z. M.; Baldini, M.; Meng, Y.; Struzhkin, V. V.; Hemley, R. J. Evidence for Superconductivity above 260 K in Lanthanum Superhydride at Megabar Pressures. *Phys. Rev. Lett.* **2019**, *122*, 027001.

(4) Zhang, W.; Oganov, A. R.; Goncharov, A. F.; Zhu, Q.; Boulfelfel, S. E.; Lyakhov, A. O.; Stavrou, E.; Somayazulu, M.; Prakapenka, V. B.; Konôpková, Z. Unexpected Stable Stoichiometries of Sodium Chlorides. *Science* **2013**, *342*, 1502−1505.

(5) Zhou, M.; Liu, S.; Du, M.; Shi, X.; Zhao, Z.; Guo, L.; Liu, B.; Liu, R.; Wang, P.; Liu, B. High-Pressure-Induced Structural and Chemical Transformations in NaN_3. *J. Phys. Chem. C* **2020**, *124*, 19904−19910.

(6) Bricker, O. Some Stability Relations in the System Mn-O_2-H_2O at 25 °C and One Atmosphere Total Pressure. *Am. Mineral.* **1965**, *50*, 1296−1354.

(7) Shang, J. F.; Zheng, F. Y. *Lange's Handbook of Chemistry (Translated version)*; Science Press: Beijing, 1991.

(8) Li, Y.; Wang, L.; Liu, H.; Zhang, Y.; Hao, J.; Pickard, C. J.; Nelson, J. R.; Needs, R. J.; Li, W.; Huang, Y.; et al. Dissociation Products and Structures of Solid H_2S at Strong Compression. *Phys. Rev. B: Condens. Matter Mater. Phys.* **2016**, *93*, 020103.

(9) Liu, G.; Besedin, S.; Irodova, A.; Liu, H.; Gao, G.; Eremets, M.; Wang, X.; Ma, Y. Nb-HSystem at High Pressures and Temperatures. *Phys. Rev. B: Condens. Matter Mater. Phys.* **2017**, *95*, 104110.

(10) Lonie, D. C.; Hooper, J.; Altintas, B.; Zurek, E. Metallization of Magnesium Poly-Hydrides under Pressure. *Phys. Rev. B: Condens. Matter Mater. Phys.* **2013**, *87*, 054107.

(11) Gao, G.; Oganov, A. R.; Bergara, A.; Martinez-Canales, M.; Cui, T.; Iitaka, T.; Ma, Y.; Zou, G. Superconducting HighPressure Phase of Germane. *Phys. Rev. Lett.* **2008**, *101*, 107002.

(12) Gao, G.; Wang, H.; Zhu, L.; Ma, Y. Pressure-Induced Formation of Noble Metal Hydrides. *J. Phys. Chem. C* **2012**, *116*, 1995−2000.

(13) Peng, F.; Sun, Y.; Pickard, C. J.; Needs, R. J.; Wu, Q.; Ma, Y. Hydrogen Clathrate Structures in Rare Earth Hydrides at High Pressures: Possible Route to Room-Temperature Superconductivity. *Phys. Rev. Lett.* **2017**, *119*, 107001.

(14) Wang, Y.; Wang, H.; Tse, J. S.; Iitaka, T.; Ma, Y. Structural Morphologies of High-Pressure Polymorphs of Strontium Hydrides. *Phys. Chem. Chem. Phys.* **2015**, *17*, 19379−19385.

(15) Ishikawa, T.; Miyake, T. Evolutionary Construction of Formation Energy Convex Hull: Practical Scheme and Application to Carbon-Hydrogen Binary System. *Phys. Rev. B: Condens. Matter Mater. Phys.* **2020**, *101*, 214106.

(16) Conway, L. J.; Hermann, A. High Pressure Hydrocarbons Revisited: FromVan Der Waals Compounds to Diamond. *Geosciences (Basel, Switz.)* **2019**, *9*, 227.

(17) Suzuki, A. Compression Behavior of Manganite. *J. Mineral. Petrol. Sci.* **2013**, *108*, 295−299.

(18) Haines, J.; Hoyau, S.; Leger, J. M.; Hoyau, S. Second-Order Rutile-Type to $CaCl_2$-Type Phase Transition in β-MnO_2 at High Pressure. *J. Phys. Chem. Solids* **1995**, *56*, 965−973.

(19) Hubbard, C. R.; Snyder, R. L. RIR-Measurement and Use in Quantitative XRD. *Powder Diffr.* **1988**, *3*, 74−77.

(20) Irvine, J. T. S.; Sinclair, D. C.; West, A. R. Electroceramics: Characterization by Impedance Spectroscopy. *Adv. Mater.* **1990**, *2*, 132−138.

https://doi.org/10.1021/acs.jpclett.1c03382
J. Phys. Chem. Lett. 2021, 12, 10893−10898